

Journal Pre-proof

IFN γ -producing CD8⁺ tissue resident memory T cells are a targetable hallmark of immune checkpoint inhibitor-colitis

Sarah C. Sasson, Stephanie M. Slevin, Vincent TF. Cheung, Isar Nassiri, Anna Olsson-Brown, Eve Fryer, Ricardo C. Ferreira, Dominik Trzuppek, Tarun Gupta, Lulia Al-Hillawi, Mari-Ienna Issaias, Alistair Easton, Leticia Campo, Michael EB. FitzPatrick, Joss Adams, Meenali Chitnis, Andrew Protheroe, Mark Tuthill, Nicholas Coupe, Alison Simmons, Miranda Payne, Mark R. Middleton, Simon PL. Travis, The Oxford IBD Cohort Investigators, Benjamin P. Fairfax, Paul Klenerman, Oliver Brain

PII: S0016-5085(21)03139-5
DOI: <https://doi.org/10.1053/j.gastro.2021.06.025>
Reference: YGAST 64414

To appear in: *Gastroenterology*
Accepted Date: 8 June 2021

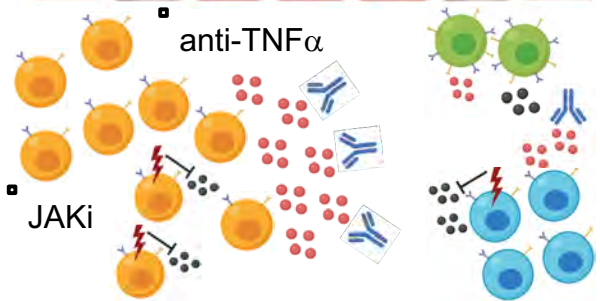
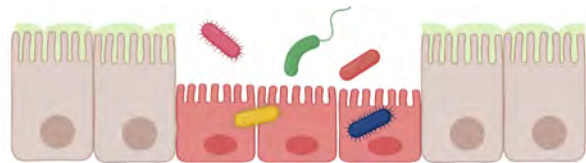
Please cite this article as: Sasson SC, Slevin SM, Cheung VT, Nassiri I, Olsson-Brown A, Fryer E, Ferreira RC, Trzuppek D, Gupta T, Al-Hillawi L, Issaias M-I, Easton A, Campo L, FitzPatrick ME, Adams J, Chitnis M, Protheroe A, Tuthill M, Coupe N, Simmons A, Payne M, Middleton MR, Travis SP, The Oxford IBD Cohort Investigators, Fairfax BP, Klenerman P, Brain O, IFN γ -producing CD8⁺ tissue resident memory T cells are a targetable hallmark of immune checkpoint inhibitor-colitis, *Gastroenterology* (2021), doi: <https://doi.org/10.1053/j.gastro.2021.06.025>.

This is a PDF file of an article that has undergone enhancements after acceptance, such as the addition of a cover page and metadata, and formatting for readability, but it is not yet the definitive version of record. This version will undergo additional copyediting, typesetting and review before it is published in its final form, but we are providing this version to give early visibility of the article. Please note that, during the production process, errors may be discovered which could affect the content, and all legal disclaimers that apply to the journal pertain.

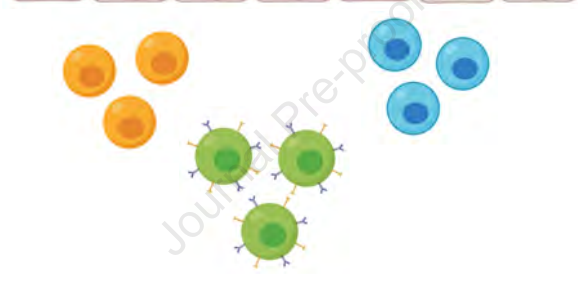
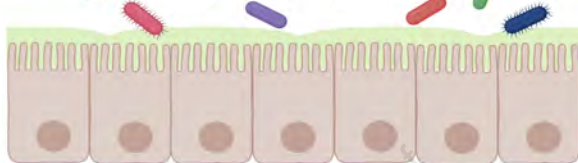
© 2021 by the AGA Institute



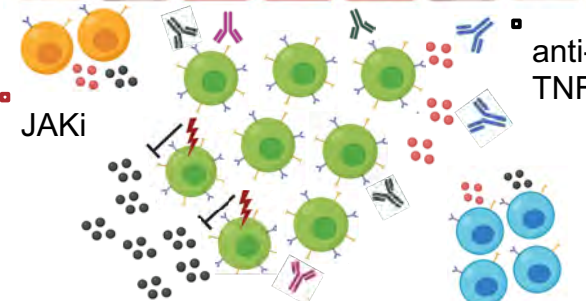
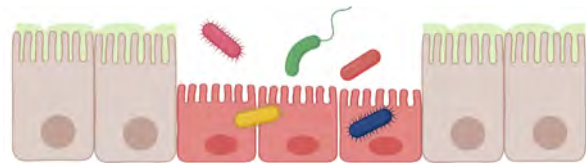
Ulcerative colitis



Healthy colon



ICI-induced colitis



CD4⁺ CD8⁺ T_{RM}

PD-1

TNF α

anti-CTLA4

JAK inhibitor (JAKi)

Conventional CD8⁺

CTLA-4

IFN γ

anti-PD1

anti-TNF α

Gastroenterology

IFN γ -producing CD8⁺ tissue resident memory T cells are a targetable hallmark of immune checkpoint inhibitor-colitis

Sarah C Sasson^{1,2}, Stephanie M Slevin^{1,2#}, Vincent TF Cheung^{1,2#}, Isar Nassiri^{3#}, Anna Olsson-Brown^{4,5}, Eve Fryer⁶, Ricardo C Ferreira⁷, Dominik Trzupek⁷, Tarun Gupta^{1,3}, Lulia Al-Hillawi^{1,2}, Mari-lenna Issaias⁸, Alistair Easton⁶, Leticia Campo⁹, Michael EB FitzPatrick^{1,2}, Joss Adams¹⁰, Meenali Chitnis⁸, Andrew Protheroe⁸, Mark Tuthill⁸, Nicholas Coupe⁸, Alison Simmons^{1,3}, Miranda Payne⁸, Mark R Middleton^{2,8}, Simon PL Travis^{1,2}, The Oxford IBD Cohort Investigators, Benjamin P Fairfax^{3,8}, Paul Klenerman^{1,2} and Oliver Brain^{1,2*}

#Equal second authors

1. Translational Gastroenterology Unit, John Radcliffe Hospital, University of Oxford, Oxford, United Kingdom.
2. NIHR Oxford Biomedical Research Centre, Oxford University Hospitals NHS Foundation Trust, John Radcliffe Hospital, Oxford, United Kingdom.
3. MRC Human Immunology Unit, MRC Weatherall Institute of Molecular Medicine, John Radcliffe Hospital, University of Oxford, Oxford, United Kingdom
4. Institute of Translational Medicine, University of Liverpool, Liverpool, United Kingdom.
5. The Clatterbridge Cancer Centre NHS Foundation Trust, Wirral, United Kingdom
6. Department of Cellular Pathology, Oxford University Hospitals NHS Foundation Trust, John Radcliffe Hospital, Oxford, United Kingdom
7. Wellcome Centre for Human Genetics, Nuffield Department of Medicine, NIHR Oxford BRC, University of Oxford, Oxford, United Kingdom
8. Department of Oncology, University of Oxford and Oxford Cancer Centre, Churchill Hospital, Oxford University Hospitals NHS Foundation Trust, Oxford, United Kingdom.

9. Translational Histopathology Laboratory, Department of Oncology, University of Oxford, United Kingdom.
10. Berkshire Cancer Centre, Royal Berkshire Hospital, Reading, United Kingdom

Grant support

SCS and SMS are supported by an Oxford-BMS Postdoctoral Fellowship. VTFC is supported by a Norman Collisson Foundation Fellowship and an Oxford Health Services Research Committee (OHSRC) grant. RCF and DT are supported by a strategic award and grant from the Juvenile Diabetes Research Foundation (4-SRA-2017-473-A-A and 1-SRA-2019-657-A-N) and the Wellcome Trust (107212/A/15/Z). PK is supported by the Wellcome Trust (WT109965MA), NIH U192U19AI082630 and is an NIHR Senior Fellow. OB, BPF and MRM receive support from Oxford NIHR BRC. The Translational Histopathology Laboratory is funded by the Experimental Cancer Medicines Centres. Reagents for the Nanostring experiments were provided as part of a Nanostring grant. The views expressed are those of the authors and not necessarily those of the NHS, the NIHR or the Department of Health.

Abbreviations

CTLA-4	cytotoxic T-lymphocyte-associated protein 4
DCC	anti-CTLA-4/PD-1 dual checkpoint inhibitor-colitis
DCNC	anti-CTLA-4/PD-1 dual checkpoint inhibitor no-colitis
FMT	fecal microbiota transplant
HV	healthy volunteer(s)
ICI	immune checkpoint inhibitor
IFNG	interferon gamma

JAK	janus kinase
mAb	monoclonal antibody
NSCLC	Non-small-cell lung cancer
PD-1	programmed cell death protein 1
PDC	anti-PD-1-monotherapy colitis
PDNC	anti-PD-1-monotherapy no-colitis
STAT	signal transducer and activator of transcription
T_{RM}	tissue resident memory T cell
TIL	tumor infiltrating lymphocyte
UCEIS	ulcerative colitis endoscopic index of severity

Corresponding author:

Dr Oliver Brain

Translational Gastroenterology Unit, Nuffield Department of Medicine

Level 5, John Radcliffe Hospital, Oxford, United Kingdom OX3 9DU

Phone: +44 1865225543 email: oliver.brain@ouh.nhs.uk

Disclosures

There are no author conflicts of interest in relation to the content of the manuscript.

Author Contributions

SCS, PK and OB designed the project. SCS, SMS, RF and MEBF performed wet-laboratory experiments. IN, DT and BF performed computational analysis. EF, AE and LC performed histological scoring. VTFC and OB performed endoscopic scoring and obtained biopsy samples. SCS, SMS, VTFC, AOB and TG collected clinical samples. VTFC, L A-H, MI, JA,

MC, AP, MT, NC, MP, MM, SPLT and OB cared for patients and facilitated translational research. AS, BF, PK and OB supervised researchers. SCS, SMS, PK, VTFC and OB wrote the manuscript. All authors reviewed and edited the final manuscript.

Acknowledgements

We thank the patients for their generous participation in this study. Thanks also to James Chivenga and the Oxford Translational Gastroenterology Unit Biobanking team for assistance with biopsy collection. Thank you to Dr Helen Ferry and Liam Hardy for assistance with cell-sorting experiments, and to Dr Joanna Hester and Jim White for assistance and expertise with Nanostring. We acknowledge Dr Rubeta Matin, who provides dermatological care to the melanoma patients.

Abstract:**Background and aims**

The pathogenesis of immune checkpoint inhibitor (ICI)-colitis remains incompletely understood. We sought to identify key cellular driver(s) of ICI-colitis and their similarities to idiopathic ulcerative colitis (UC), and to determine potential novel therapeutic targets.

Methods

We used a cross-sectional approach to study patients with ICI-colitis, those receiving ICI without the development of colitis, idiopathic UC and healthy controls. A subset of ICI-colitis patients were studied longitudinally. We applied a range of methods including multi-parameter and spectral flow cytometry, spectral immunofluorescence microscopy, targeted gene panels, bulk and single-cell RNASeq.

Results

We demonstrate CD8⁺ tissue resident memory T (T_{RM}) cells are the dominant activated T cell subset in ICI-colitis. The pattern of gastrointestinal immunopathology is distinct from UC at both the immune and epithelial-signalling level. CD8⁺ T_{RM} cell activation correlates with clinical and endoscopic ICI-colitis severity. scRNASeq analysis confirms activated CD8⁺ T_{RM} cells express high levels of transcripts for checkpoint inhibitors and *IFNG* in ICI-colitis. We demonstrate similar findings in both anti-CTLA-4/PD-1 combination therapy, and in anti-PD-1 inhibitor-associated colitis. On the basis of our data we successfully targeted this pathway in a patient with refractory ICI-colitis, using the JAK inhibitor tofacitinib.

Conclusion

IFN γ -producing CD8⁺ T_{RM} cells are a pathological hallmark of ICI-colitis, and a novel target for therapy.

Keywords: immunotherapy colitis; checkpoint colitis; ulcerative colitis; tofacitinib

Introduction

Immune checkpoint inhibitors (ICI) are revolutionising the treatment of melanoma and other cancers but come at the cost of immune-related adverse events (irAE). These irAE commonly affect the gastrointestinal (GI) tract, with those receiving combination anti-CTLA-4 and PD-1 therapy displaying increased rates of ICI-colitis (32-37%) compared to those treated with anti-PD-1 monotherapy (4-6%)^{1,2}. There is a higher incidence of ICI-diarrhea (44%)¹, probably due to unconfirmed colitis. ICI-colitis results in the greatest overall mortality of irAE, although other rarer toxicities (e.g. myocarditis) have lower individual survival rates³.

Current management for ICI-colitis includes systemic corticosteroids, and subsequent anti-TNF α therapy (infliximab) for inadequately controlled disease⁴. Alternative therapies include anti- $\alpha 4\beta 7$ integrin (vedolizumab)⁵, and fecal microbiota transplant (FMT)⁶. These therapeutic approaches are empirically derived from the treatment of idiopathic inflammatory bowel disease (IBD), without an understanding of how analogous this newer entity is to more classical forms of colitis. Refractory cases of ICI-colitis occur, resulting in steroid toxicity and, on occasion, colectomy. It is anticipated that greater insight into the mechanisms underlying ICI-colitis will lead to more targeted treatments. ICI-colitis is heterogeneous but can mimic UC and, less commonly, Crohn's disease⁷. We opted to use UC as the external disease control as both conditions typically affect the rectum and/or sigmoid colon and are amenable to flexible sigmoidoscopy.

At the outset of this study little was known about the cellular and molecular pathogenesis of ICI-colitis. The available data suggested that anti-CTLA-4-associated colitis is associated with CD8⁺ T cells⁸ and an upregulation of Th1 and Th17 effector pathways including *IFNG*⁹. We previously demonstrated that anti-CTLA-4/PD-1 colitis is associated with high levels of activated (HLA-DR⁺CD38⁺) memory CD8⁺ T cells¹⁰, and lower proportions of regulatory T cells compared with UC¹⁰. We hypothesised that CD8⁺ T_{RM} are

implicated in the pathogenesis of ICI-colitis, postulating they would become activated in an off-target consequence, and sought to understand the signalling pathways involved (see Study Design, figure 1).

T_{RM} cells are specialist lymphocytes enriched at mucosal sites including the gut¹¹, and display minimal circulation. $CD8^+ T_{RM}$ cells classically express CD69 and CD103, and play an important role in mucosal immunity (reviewed in¹²). They are implicated in the pathogenesis of autoimmune skin conditions¹³. T_{RM} -like tumor infiltrating lymphocytes (TILs) also mediate anti-tumor responses^{14,15}, and a higher proportion of T_{RM} -like TILs correlates with disease-free survival¹⁶⁻¹⁷. T_{RM} -like TILs express high levels of checkpoint proteins¹⁸⁻²⁰, which appear to act primarily as negative regulators rather than markers of exhaustion.

Recent data utilised single cell technology to identify cytotoxic $CD8^+$ T cells as the main pathogenic GI population in anti-CTLA-4/PD-1-colitis²¹. It was inferred through T cell receptor sequence analysis that these may in part derive from T_{RM} cells. Upregulation of both *IFNG* and *TNFA* signalling pathways was identified in the $CD4^+$ and $CD8^+$ T cells of ICI-colitis patients, acting on the myeloid cellular compartment²¹. Our study supports and extends the prior analysis via a broader range of experimental techniques. We also provide a direct comparison with idiopathic UC and, include analysis of anti-PD-1 monotherapy colitis and anti-CTLA-4/PD-1-gastritis. Our data taken together directly implicate *IFNG*-expressing $CD8^+ T_{RM}$ cells as a major pathogenic T cell population in the colon.

Finally, on the basis of our laboratory data we predicted that tofacitinib would be an effective therapy in a case of refractory anti-PD-1-colitis and used this successfully. These data, consistent with the subsequently published case reports of successful tofacitinib therapy^{22,23}, provide compelling insights into the underlying pathogenic mechanisms in this clinical setting and novel pathways to target therapeutically.

Materials and Methods

Subjects

We studied patients with anti-CTLA-4/PD-1-colitis (“dual checkpoint inhibitor colitis” DCC; N=15), anti-CTLA-4/PD-1 treated with no colitis (DCNC; N=10), anti-PD-1-colitis (PDC; N=6), and anti-PD-1 treated with no colitis (PDNC; N=5); active UC (disease flare assessment; N=10) and Healthy Volunteers (N=22). The UC and ICI-colitis patients are reasonably matched in terms of inflammation severity, and previous and current therapy, but do have a longer median acute flare duration in the UC cohort (see supplementary table 1), and the usual caveats must apply when interpreting real-world human data from subjects that are not perfectly aligned. All patients provided written informed consent for participation (Oxford GI Illness Biobank 16/YH/0247 or PRedicting Immunotherapy Side Effects “PRISE” study London-Surrey Research Ethics Committee: REC18/LO/0412). This consent enabled invitation for sigmoidoscopy pre-ICI, at Week 5-7 post ICI-treatment and at the development of colitis symptoms (see figure 1). Colitis disease activity is comparable across UC and ICI-colitis. The duration of active colitis and the treatment at the time of sampling are detailed (supplementary table 1). Rectal and sigmoid biopsies were protocolised. Individual patient samples studied in each experiment are shown in supplementary table 2.

The clinical characteristics of patients with anti-CTLA-4/PD-1-associated gastritis (DCG; N=4) and healthy volunteer controls (N=7) are shown in supplementary table 3.

Isolation of mononuclear cells from gastrointestinal tissue

Colonic biopsies were placed in RPMI media containing penicillin and streptomycin and 10% foetal calf serum. Biopsies underwent enzymatic and mechanical digestion with 1mg/mL Collagenase D (Sigma-Aldrich) and 100µg/mL DNase I (ThermoFisher) and

shaken at 37°C for 1h. Biopsies were dissociated using gentleMACS Dissociator (Miltenyi Biotech) and passed through a 70µm strainer.

Flow cytometry

Flow cytometry was performed on freshly isolated mononuclear cells, using a near infra-red live/dead stain (Invitrogen) and an initial monoclonal antibody (mAb) panel (see supplemental methods) was performed on a three-laser LSR Fortessa X-20 (BD Biosciences). An extended T_{RM} cell phenotyping mAb panel (see supplemental methods) was performed on an Aurora spectral analyser (Cytex).

Data was analysed using FACSDIVA v8.0.1 software (BD Biosciences). Gating strategies are shown in supplementary figure 2A. Lymphocyte populations are reported as a proportion of parent populations.

Statistics

Differences between groups were determined using the unpaired non-parametric Mann-Whitney test. Correlation analysis was performed using the non-parametric Spearman's test. All were performed using SPSS software (IBM, NY, USA). Medians and interquartile ranges are reported throughout. A *P* value < .05 was considered statistically significant. Where multiple comparisons were performed a Bonferroni correction was made (see individual figure legends).

Multiplex immunofluorescence microscopy

Multiplex immunofluorescence staining was carried out on 4µm formalin fixed paraffin embedded sections using the OPAL™ protocol (AKOYA Biosciences) on the Leica BOND RX^m autostainer (Leica, Microsystems). Six consecutive staining cycles were

performed using primary antibody-Opal fluorophore pairings. Whole slide scans and multispectral images (MSI) were obtained on the AKOYA Biosciences Vectra® Polaris™. Batched analyzed MSIs were fused in HALO (Indica Labs), to produce a spectrally unmixed reconstructed whole tissue image.

Nanostring RNA plex

Targeted gene expression was measured using 150µg of RNA extracted from pinch biopsies and a 770-gene human autoimmune profiling panel with a custom 10-gene spike in set (supplemental methods). Samples were analysed on an nCounter Sprint profiler with downstream analysis using nSolver freeware (Nanostring), Gene Set Enrichment Analysis (Broad Institute) and R studio (Boston).

Bulk RNASeq

Bulk RNASeq analysis was performed using 900ng per sample of RNA extracted from pinch biopsies and the GRCH37.EBVB95-8wt reference genome. Total RNA was converted to cDNA with second strand cDNA incorporating a dUTP. cDNA was end-repaired with PolyA tails and was adapter-ligated. Sequencing was performed on a NovaSeq6000 (Illumina). Bulk RNASeq was analysed using Partek Flow software. Library generation and sequencing were performed at the Oxford Genomics Centre. Data analysis was performed according to published standards^{24 25 26 27}.

10X Genomics library preparation and sequencing

scRNAseq libraries were generated using 10X Genomics Chromium scRNA Reagents Kits (v1 Chemistry). Live CD45⁺ cells were sorted using a FACSAriaIII cell sorter (BD Biosciences) and resuspended in PBS with 0.04% BSA at ~1000 cells/µL and loaded onto

two lanes of the Chromium Controller. Captured cell number was 5,876. Library quality and concentration was determined using a TapeStation (Agilent) and Qubit 2.0 Fluorometer (Thermo Fisher). Libraries were sequenced on an Illumina HiSeq 4000 to a mean depth of 64,000 mean reads/cell. Library generation and sequencing were performed at the Oxford Genomics Centre.

Droplet-based (10X Genomics) scRNAseq data analysis

FastQ generation, read alignment, barcode counting, and UMI counting was performed using the Cell Ranger pipeline v2.2.0. Downstream processing steps were performed using Seurat v2.3.4. Genes expressed in fewer than 10 cells, were removed. Cells with a local minimum of the UMI distribution to the left of the mode UMI count, < 500 genes, and >10,000 UMIs, > 2500 genes, and/or > 10% mitochondrial reads were removed. Data were log normalised and scaled, with cell-cell variation due to UMI counts, percent mitochondrial reads, and S and G2M cell cycle scores regressed out.

Genetic de-multiplexing single-cell RNA-sequencing

Demultiplexing single-cell RNA-sequencing was run with the inferred genotypes from the bulk RNAseq data that we have sequenced as part of this same project. We used the GATK variant calling pipeline on the samples included in each pool (GX06/GX18) and fed that to demuxlet as described in²⁸.

scRNASeq data processing and quality control

Cellranger (v 3.0.2) mkfastq was applied to the Illumina BCL output to produce FASTQ files. Cellranger count was then applied to each FASTQ file to produce a feature

barcoding and Gene expression library. Cellranger aggr was used to combine samples for merged analysis.

We applied *scater* package to filter out single-cell profiles that were outliers for any metric, as low-quality libraries²⁹. Data analysis was performed according to published standards^{30 31 32 33}. All datasets used and additional scripts are available online (<https://bitbucket.org/Fairfaxlab/prise-sarah-sassion/src/master/>).

Identification T cell clusters

We used the “Area Under the Curve” (AUC) to calculate whether a T cell reference gene set was enriched within the expressed genes for each cell³⁴. We used the Human Protein Atlas database reference gene list for T cells, downloaded from (<https://www.proteinatlas.org/humanproteome/blood/blood+cells+summary> *cell type group enriched genes*). The repository is provided as supplementary file (**repository_reference_gene_sets.txt**).

Single-cell protein and RNASeq expression

Live CD45⁺CD3⁺ T cells were sorted using a FACSAriaIII cell sorter (BD Biosciences). A total of 46,000 T cells were sorted and stained with a cocktail of 70 oligo-conjugated AbSeq antibodies (BD Biosciences; see supplementary table 4) for 45min at 4°C. Cells were then washed to remove residual unbound AbSeq antibodies and loaded onto three BD Rhapsody cartridges (BD Biosciences) for single-cell capture.

cDNA library preparation and sequencing

Single-cell capture and cDNA library preparation were performed using the BD Rhapsody Express Single-cell analysis system (BD Biosciences) and a customised T cell expression

panels (supplementary Table 5), according to the manufacturer's instructions (for further details including data analysis and QC see supplemental methods).

Results

The majority of activated colon CD8⁺ T cells in anti-CTLA-4/PD-1 colitis are T_{RM} cells.

We previously demonstrated that the majority of T cells in the colon of ICI-colitis were CD8⁺¹⁰. We sought to determine whether these CD8⁺ T cells had a T_{RM} cell phenotype. We found that both UC and dual checkpoint inhibitor-colitis (DCC) groups are associated with increased proportions of CD3⁺ T cells in the affected tissue as compared with healthy gut, and dual checkpoint inhibitor-no-colitis (DCNC) groups, respectively (figure 2Ai). Compared with UC, DCC is associated with proportionately fewer CD4⁺ T cells and more CD8⁺ T cells (figure 2Aii-iii). The proportion of CD8⁺CD103⁺ T cells is lower in active UC compared with healthy volunteers (HV) (figure 2Aiv). Patients with DCC have a very high proportion of activated CD8⁺CD103⁺ T cells, as defined by the co-expression of HLA-DR and CD38 (median 65% of CD8⁺CD103⁺ T cells), and this is higher than in DCNC (3%; $P < .0001$) and UC (13%; $P < .01$) groups (figure 2Avi). There is some activation of CD8⁺103⁻ “non-tissue-resident” T cells in DCC compared with DCNC, however the proportion is much lower than in the CD103⁺ subset (figure 2Av). We used a more stringent definition of CD8⁺ T_{RM} cells i.e. co-expression of CD69 and CD103 to confirm high levels of cellular activation of CD8⁺ T_{RM} cells in DCC compared with DCNC (figure 2Avii-viii).

Higher cellular activation of CD103⁺CD69⁺ CD8⁺ T_{RM} cells compared to CD103⁻ CD8⁺ T cells was detected across all patient groups and is represented in figure 1A ix.

The proportion of activated colon CD8⁺ T_{RM} cells correlates longitudinally with clinical and endoscopic findings.

We investigated whether the proportion of activated CD8⁺ T_{RM} cells in the colon was an accurate biomarker of the presence of DCC, and response to therapy. Overall, CD8⁺ T_{RM} cell activation positively correlates with endoscopic severity of DCC using the Ulcerative Colitis Endoscopic Index of Severity (UCEIS) score (figure 2B). UCEIS score details are in supplementary figure 1. We previously reported that UCEIS can be used as an objective endoscopic marker of ICI-colitis clinical outcomes². We confirmed by multiplexed spectral fluorescence microscopy that in DCC, CD8⁺ T_{RM} cells reside both in gastrointestinal crypts and in the lamina propria (figure 2C).

We investigated whether activation of CD8⁺ T_{RM} cells was a phenomenon specific to ICI-colitis or was evident in other forms of irAE such as ICI-gastritis (figure 2Di). CD8⁺ T_{RM} comprise the majority of T cells in the gastric mucosa in both health and anti-CTLA-4/PD-1-gastritis (figure 2Dii-iii). The proportion of activated CD8⁺ T_{RM} was low in health (<1%; figure 2Div) and increased in anti-CTLA-4/PD-1-gastritis (30-51%; figure 2Div).

We performed an extended flow cytometric panel to further characterise the CD8⁺ T_{RM} cells in anti-CTLA-4/PD-1-colitis (supplementary figure 2B).

Anti-CTLA-4/PD-1-colitis has a transcriptome distinct from UC with up-regulated IFNG signalling.

We performed a 780-gene autoimmune profiling panel using colonic RNA to determine unique and common features between DCC, DCNC and UC groups. A heatmap of the top 50 defining features demonstrates that DCC is associated with upregulated *STAT1*, *GBP2*, *IFI30*, *GZMB*, *PSMB9*, *IFITM1*, *HLAB*, *S100A9* and *CXCL1* (figure 3A).

We identified 259 genes that are upregulated more than 2-fold across the DCC, DCNC and UC groups when compared to HV (figure 3B). Of the 173 genes upregulated in DCC, only 12/173 are common to the DCNC group, indicating these changes are not simply

an on-treatment effect. Of the 173 genes upregulated in DCC, 144/173 are in common with UC, and 29 are unique (figure 3B).

Exploration of the 173 upregulated genes in DCC using g:Profiler pathway analysis highlights a number of biological pathways (figure 3C). The top 30 pathways include defense response, response to external biotic stimulus and cytokine-mediated pathways. The most pathway-specific results include a response/ cellular response to IFN γ (figure 3C; supplementary table 6). We confirm that the canonical JAK/STAT components of IFN γ signalling are upregulated in anti-CTLA-4/PD-1-colitis compared to controls (figure 3D).

Volcano plots showing differentially expressed genes in UC versus HV, DCC versus DCNC, and DCC versus UC are shown in supplementary figure 3. Up-regulated genes common to DCC and UC include *S100A8*, *S100A9* and *IDO1*. DCC is associated with lower expression of canonical B cell markers CD19, MS4A1(CD20) and CD22 compared to UC.

Bulk RNASeq analysis confirms a distinct transcriptome for anti-CTLA-4/PD-1 associated colitis enriched for IFNG signalling.

RNASeq analysis from bulk RNA extracted from colonic biopsies confirms the transcriptomic signature associated with DCC is distinct from UC (figure 4A-B). As opposed to the Nanostring panel, which selects for genes expressed by lymphocytes, the bulk RNASeq analysis is predominated by epithelial signals. Analysis of modular hallmark gene sets demonstrates patients with DCC have highly expressed *IFNG* response, in excess of *TNFA* signalling (figure 4C).

Single cell RNASeq confirms anti-CTLA-4/PD-1-colitis is associated with high proportions of activated CD8⁺ T_{RM} cells that express transcripts for CTLA-4, PD-1, TIGIT, TIM-3, LAG-3 and IFNG.

Single cell analysis formed 8 main clusters (figure 5A) that include T cells (Clusters 2,4,5), B cells (Cluster 1,6,8), Plasmablasts (Cluster 7) and monocytes (Cluster 3). UC has a higher proportion of B cells and plasmablasts compared with ICI-colitis groups and HV (figure 5B). The defining features of each cluster are shown in figure 5C and supplementary table 7. Co-expression of *ITGAE* (*CD103*) and *CD69* is strongest in Cluster 4 and identifies cells with a T_{RM} cell phenotype. The DCC group has the highest proportion of cells with a T_{RM} cell phenotype (Cluster 4; figure 5B). These cells have a very high expression of immune checkpoint transcripts including *CTLA4*, *PDCD1* (*PD-1*), *TIGIT*, *HAVCR2*(*TIM-3*) and *LAG3*, which are minimally detected or absent in the other clusters (figure 5D).

We further investigated the T cell component of the scRNAseq dataset (figure 5E and G). $CD8^+$ T cells with a T_{RM} cell phenotype can be identified as cells co-expressing transcripts for *CD8A*, *CD8B*, *ITGAE* and *CD69* (figure 5F) and there is evidence for these cells expressing high amounts of *HLADR*, *GZMB* and *PRF1* (figure 5H). We have demonstrated by Nanostring and bulk RNASeq that $IFN\gamma$ signalling pathways are enriched in anti-CTLA-4/PD-1-colitis, but the source of *IFNG* message cannot be determined at a bulk RNASeq level. Utilising scRNASeq we are able to confirm *IFNG* production in T cells that overlap with the T_{RM} cell zones (figure 5F and I) and that *IFNG* production is detected in all UC, DCC and anti-PD-1-colitis (PDC) groups (figure 5I).

Heat map analysis demonstrates that each group has a distinct set of upregulated genes (figure 5J). T cells from patients with DCC have significantly higher expression of *MT2A*, *S100A11*, *GNLY*, *MT1E*, *GZMB* and *CCL20*. T cells from patients with PDC have significantly higher expression of *DUSP4*, *NR3C1*, *HLADPB1*, *HLADR85* and *HSPA1A*. T cells from patients with UC have significantly higher expression of *SELL*, *CCR7*, *IFITM3*, *FAM118A* and *FCMR*.

The defining characteristics of ITGAE⁺(CD103⁺) colonic T cells (as compared to ITGAE⁻ T cells) are shown in figure 5K. These cells have significantly higher expression of *CCL5*, *NKG7*, *CD8A*, *GZMA*, *TMIGD2*, *TNFRSF9*, *GZMB*, *GNLY*, *IFNG*, *CXCR6*, *LAG3* and *TIGIT* and lower expression of *CCR7*, *CD28* and *CD4*.

To confirm our finding that CD8⁺ T_{RM} cells display high expression of *IFNG*, including in patients with PDC, we performed a second single-cell protein and RNASeq experiment, this time sorting on live CD45⁺CD3⁺ T cells (Figure 6). The cells form 7 clusters (Figure 6A and supplementary table 8) including 3 clusters of CD8⁺ T_{RM} cells (Clusters 1,2 and 6), a tissue-resident CD4⁺ T cell population (Cluster 4) and 3 populations of non-resident classical T cells (Cluster 0, 3 and 5). There is a clear separation of CD4⁺ (Figure 6B) and CD8⁺ T cell populations (Figure 6C), with CD103(ITGAE) predominantly overlapping with CD8⁺ T cells (Figure 6D). Co-expression of CD8, CD103(ITGAE) and CD69 defines the CD8⁺ T_{RM} cell clusters (Figure 6E). Expression of *IFNG* overlaps with CD8⁺ T_{RM} cell populations and, to a lesser degree, the CD4⁺CD103⁺ T cells (Figure 6F). T cells from patients with PD-1 colitis are predominantly in the CD8⁺ T_{RM} cell populations (Cluster 1 and 6) and are distinct from T cells from active UC which are predominantly in the conventional and CD4⁺ T cell zones (Figure 6G).

We extracted data pertaining to the 3 CD8⁺ T_{RM} cell populations (figure 6H), and find that the CD8⁺ T_{RM} cell Population 2, comprised mostly from cells from patients with PD-1-colitis, has markedly high expression of activation markers (*HLADR*, *CD38*) and checkpoint molecules (*CTLA4*, *TIM3*). This transcriptome is distinct from CD8⁺ T_{RM} cell Population 1, which has a greater representation in health and expresses high levels of *IL7R* and *CCL4*. The smaller CD8⁺ T_{RM} cell Population 3 again contains unique features including *KIR2DL4*, *KLRC3* and includes a $\gamma\delta$ T cell component.

Tofacitinib results in rapid resolution of treatment-refractory anti-PD-1 associated colitis and reversal of CD8⁺ T_{RM} cell activation and IFN γ -signalling.

A 61-year-old man with metastatic NSCLC was treated with combination chemotherapy (carboplatin and pemetrexed) and pembrolizumab (see figure 7A). After 2 cycles he developed symptoms of ICI-colitis, confirmed endoscopically and histologically. (UCEIS and Nancy score details are in supplementary figure 1.) He did not respond to IV steroids or two doses of infliximab. We had previously seen a rapid resolution of refractory anti-CTLA-4/PD-1 colitis with FMT treatment in a different patient, with corresponding decreases in CD8⁺ T_{RM} cell activation (figure 7B). We prioritised FMT over vedolizumab as he required rapid induction therapy. There was a modest initial clinical response to FMT, however on follow-up sigmoidoscopies over the subsequent 12 weeks he continued to have refractory colitis of an equivalent endoscopic and histologic severity. This was confirmed by flow cytometry (figure 7C). Our data collectively provided us with evidence that tofacitinib, a JAK inhibitor, was a potential therapeutic option. After discussion with the patient, tofacitinib was prescribed at 10mg BD, with concomitant venous thromboembolism prophylaxis³⁵. He made an immediate clinical response and achieved endoscopic and histologic remission by 5 weeks (figure 7A), commensurate with resolution of activated CD8⁺ T_{RM} cells (61% to 7%; figure 7D). Tofacitinib was ceased after 6 weeks, and he restarted chemotherapy. He has made a good oncological response, and 10 months later colitis has not recurred.

An RNA-plex assay of colonic mucosal RNA pre- and post-tofacitinib therapy shows down-regulation of key JAK-STAT signalling components known to be down-stream of IFN γ signalling (figure 7F). The overall transcriptional response to tofacitinib therapy demonstrates down-regulation of transcripts including *S100A8*, *IDO1*, *S100A9* (figure 7G).

Discussion

The profound success of ICIs has resulted in broader applications, and an increasing incidence of ICI-colitis which is frequent and has the greatest overall irAE mortality³.

Here we present a comprehensive analysis of ICI-colitis utilising multi-parameter and spectral flow cytometry, RNA-plex, bulk and single cell analysis. We find that in all patient groups the majority of colon-derived CD8⁺ T cells are T_{RM} cells, and that in anti-CTLA-4/PD-1-colitis the highest activation levels are seen in T_{RM} cells. CD8⁺ T_{RM} cell activation anti-CTLA-4/PD-1 colitis correlates with clinical, endoscopic and histopathological findings, and the response to treatment over time. Additionally, CD8⁺ T_{RM} cell activation is also present in ICI-gastritis, which involves a distinct epithelium and microenvironment from the colon, and this may have implications for the pathogenesis of extra-gastrointestinal irAEs.

We have made a direct comparison with active UC and find that the level of CD8⁺CD103⁺ T cell activation is significantly greater in the DCC group. We identify both the immunological commonalities with UC, and disparate features. In addition to differences in T cell populations, we demonstrate that B lineage populations are over-represented in the UC samples and comparatively absent in ICI-groups, indicating that pathogenic B cells likely play a smaller role in ICI-colitis. The *IFNG*-response pathway is upregulated in both UC and DCC, but with an enhanced activation in both DCC and PDC indicating that targeting this pathway may be even more effective in ICI-colitis.

Our scRNASeq experiments confirm that CD8⁺ T_{RM} cells are enriched in ICI-colitis, and display the highest proportion of immune checkpoint transcripts, including CTLA4 and PCDC1 (PD-1). This supports recently published data²¹ and provides a likely mechanism by which these cells become disproportionately and rapidly activated after ICI administration. We confirm that the production of *IFNG* clusters in the same region as CD8⁺ T_{RM} cells, extending the data from Luoma *et al* which identified *IFNG* and *TNFA* upregulation in the CD4⁺ and CD8⁺ T cells, and acting on the myeloid cellular compartment²¹. Our analysis of

ITGAE(CD103)⁺ T cells reveals an expression profile similar to CD8⁺ T_{RM} cells in vitiligo¹³, with 5 upregulated genes that largely relate to cytotoxicity featuring in both datasets: *GZMB*, *GNLY*, *NKG7*, *CCL5*, *IFNG*. Our data suggest that in health CD8⁺ T_{RM} cells express a homeostatic signature including *IL7R*, but that in ICI-associated colitis there is significant upregulation of activation molecules and checkpoint molecules.

We find compelling evidence for upregulated *IFNG* signalling in ICI-colitis, more so than *TNFA* which is the current target of ICI-colitis rescue therapy. We present a patient with refractory ICI-colitis who we successfully treated with tofacitinib, and with robust resolution of CD8⁺ T_{RM} cell activation. This aligns with the recent case reports of successful tofacitinib therapy for treatment-refractory ICI-colitis^{22 23}. We acknowledge that a series of cases cannot conclusively determine a treatment's large-scale efficacy or safety. IFN γ signalling is a well-established pathway in tumor control. Early work in murine models found that neutralising IFN γ interferes with tumor rejection in immunocompetent hosts³⁶. Mice lacking *IFNG* signalling components *IFNGR1* or *STAT1* develop a higher percentage of tumors at a faster rate³⁷. We recognise concern that use of JAK inhibition in ICI-colitis may deactivate not only colonic but also intra-tumoral CD8⁺ T_{RM} cells, which are a key therapeutic target^{38 39}. In human melanoma, *IL-7* signalling⁴⁰, T cell infiltration and IFN γ signalling signatures⁴¹ have a high association with tumor response to immune checkpoint inhibitors, and conversely defects in IFN γ signalling, including loss-of function mutations in *IFNGR1*, *JAK1*, *JAK2* and *STAT1* are associated with resistance to checkpoint blockade⁴²⁻⁴⁶. Although larger clinical trials are needed to establish the safety and efficacy of tofacitinib for ICI-colitis, our analysis provides a complete bench-to-bedside cycle: from a novel disease entity, hypothesis, and mechanistic study, to intervention with a rationally re-purposed therapeutic. Our data suggest that tofacitinib may be a useful therapy in patients with refractory ICI-colitis as a salvage therapy.

Our study has limitations. We acknowledge our relatively small cohort of patients, and given the real-world nature of our study these patients are not perfectly matched. In addition the relatively low cell number in some of the experiments, notably the initial single cell RNAseq, mean that the UC and ICI-colitis comparison could bias toward commonalities. Comparison of a chronic disease (UC) with longstanding inflammatory response against an acute iatrogenic colitis may also confound the data. Whilst the UC patients do have a longer median flare duration, the cohorts are otherwise well-matched in relation to inflammation severity, and previous and current therapy (see supplementary table 1). Future studies could aim to reduce the heterogeneity of enrolled ICI-colitis and comparator where possible, and this may require larger multi-centre studies. In addition, whilst we attempted to study ICI-colitis CD8⁺ T_{RM} cells *ex vivo*, the high rates of apoptosis, in keeping with down-regulated Bcl-2 expression (see supplementary Figure 2), made this challenging. We suggest Cluster 4 in our scRNASeq experiment is likely numerically under-represented, given our flow cytometry results were conducted on fresh tissue.

There remain many unanswered questions, including what factor(s) drive a subset of patients to develop ICI-colitis, leaving others unaffected. We postulate that activated CD8⁺ T_{RM} cells in ICI-colitis are responding to commensal or pathogenic microbes, and that this results in high levels of cellular activation and IFN γ signalling that propagates downstream and widespread tissue activation. Furthermore, the use of FMT for treatment of ICI-colitis (for which we describe one treatment success) implies that replacement of the microbiome may remove the instigating antigen⁶.

Our work has identified that *IFNG* producing CD8⁺ T_{RM} cells are a cellular hallmark of ICI-colitis. This has important implications for targeted therapy for ICI-colitis, as evidenced by the successful application of a JAK-inhibitor. These findings also suggest that medications that specifically target CD103 may prove effective therapy, and note monoclonal

antibody targeting the $\beta 7$ integrin chain. Finally, our data on $CD8^+$ T_{RM} cell activation in both colon and gastric epithelium may have broader relevance for other extra-gastrointestinal irAEs.

References:

1. Larkin J, Hodi FS, Wolchok JD. Combined Nivolumab and Ipilimumab or Monotherapy in Untreated Melanoma. *N Engl J Med* 2015;373(13):1270-1.
2. Cheung VTF, Gupta T, Olsson-Brown A, et al. Immune checkpoint inhibitor-related colitis assessment and prognosis: can IBD scoring point the way? *Br J Cancer* 2020;123(2):207-15.
3. Wang DY, Salem JE, Cohen JV, et al. Fatal Toxic Effects Associated With Immune Checkpoint Inhibitors: A Systematic Review and Meta-analysis. *JAMA Oncol* 2018;4(12):1721-28.
4. Brahmer JR, Lacchetti C, Schneider BJ, et al. Management of Immune-Related Adverse Events in Patients Treated With Immune Checkpoint Inhibitor Therapy: American Society of Clinical Oncology Clinical Practice Guideline. *J Clin Oncol* 2018;36(17):1714-68.
5. Abu-Sbeih H, Ali FS, Wang X, et al. Early introduction of selective immunosuppressive therapy associated with favorable clinical outcomes in patients with immune checkpoint inhibitor-induced colitis. *J Immunother Cancer* 2019;7(1):93.
6. Wang Y, Wiesnoski DH, Helmink BA, et al. Fecal microbiota transplantation for refractory immune checkpoint inhibitor-associated colitis. *Nat Med* 2018;24(12):1804-08.
7. Soularue E, Lepage P, Colombel JF, et al. Enterocolitis due to immune checkpoint inhibitors: a systematic review. *Gut* 2018;67(11):2056-67.
8. Arriola E, Wheeler M, Lopez MA, et al. Evaluation of immune infiltration in the colonic mucosa of patients with ipilimumab-related colitis. *Oncoimmunology* 2016;5(9):e1209615.

9. Bamias G, Delladetsima I, Perdiki M, et al. Immunological Characteristics of Colitis Associated with Anti-CTLA-4 Antibody Therapy. *Cancer Invest* 2017;35(7):443-55.
10. Sasson SC, Zaunders JJ, Nahar K, et al. Mucosal-associated invariant T (MAIT) cells are activated in the gastrointestinal tissue of patients with combination ipilimumab and nivolumab therapy-related colitis in a pathology distinct from ulcerative colitis. *Clin Exp Immunol* 2020;202(3):335-52.
11. Thome JJ, Yudanin N, Ohmura Y, et al. Spatial map of human T cell compartmentalization and maintenance over decades of life. *Cell* 2014;159(4):814-28.
12. Sasson SC, Gordon CL, Christo SN, et al. Local heroes or villains: tissue-resident memory T cells in human health and disease. *Cell Mol Immunol* 2020;17(2):113-22.
13. Cheuk S, Schlums H, Gallais S  rezal I, et al. CD49a Expression Defines Tissue-Resident CD8. *Immunity* 2017;46(2):287-300.
14. Malik BT, Byrne KT, Vella JL, et al. Resident memory T cells in the skin mediate durable immunity to melanoma. *Sci Immunol* 2017;2(10).
15. Park SL, Buzzai A, Rautela J, et al. Tissue-resident memory CD8. *Nature* 2019;565(7739):366-71.
16. Ganesan AP, Clarke J, Wood O, et al. Tissue-resident memory features are linked to the magnitude of cytotoxic T cell responses in human lung cancer. *Nat Immunol* 2017;18(8):940-50.
17. Edwards J, Wilmott JS, Madore J, et al. CD103. *Clin Cancer Res* 2018;24(13):3036-45.
18. Savas P, Virassamy B, Ye C, et al. Single-cell profiling of breast cancer T cells reveals a tissue-resident memory subset associated with improved prognosis. *Nat Med* 2018;24(7):986-93.

19. Boddupalli CS, Bar N, Kadaveru K, et al. Interlesional diversity of T cell receptors in melanoma with immune checkpoints enriched in tissue-resident memory T cells. *JCI Insight* 2016;1(21):e88955.
20. Clarke J, Panwar B, Madrigal A, et al. Single-cell transcriptomic analysis of tissue-resident memory T cells in human lung cancer. *J Exp Med* 2019;216(9):2128-49.
21. Luoma AM, Suo S, Williams HL, et al. Molecular Pathways of Colon Inflammation Induced by Cancer Immunotherapy. *Cell* 2020;182(3):655-71.
22. Esfahani K, Hudson M, Batist G. Tofacitinib for Refractory Immune-Related Colitis from PD-1 Therapy. *N Engl J Med* 2020;382(24):2374-75.
23. Bishu S, Melia J, Sharfman W, et al. Efficacy and Outcome of Tofacitinib in Immune checkpoint Inhibitor Colitis. *Gastroenterology* 2021;160(3):932-34.
24. Rohart F, Gautier B, Singh A, et al. mixOmics: An R package for 'omics feature selection and multiple data integration. *PLoS Comput Biol* 2017;13(11):e1005752.
25. Russo PST, Ferreira GR, Cardozo LE, et al. CEMiTool: a Bioconductor package for performing comprehensive modular co-expression analyses. *BMC Bioinformatics* 2018;19(1):56.
26. Liberzon A, Birger C, Thorvaldsdóttir H, et al. The Molecular Signatures Database (MSigDB) hallmark gene set collection. *Cell Syst* 2015;1(6):417-25.
27. Oughtred R, Stark C, Breitkreutz BJ, et al. The BioGRID interaction database: 2019 update. *Nucleic Acids Res* 2019;47(D1):D529-D41.
28. Kang HM, Subramaniam M, Targ S, et al. Multiplexed droplet single-cell RNA-sequencing using natural genetic variation. *Nat Biotechnol* 2018;36(1):89-94.
29. McCarthy DJ, Campbell KR, Lun AT, et al. Scater: pre-processing, quality control, normalization and visualization of single-cell RNA-seq data in R. *Bioinformatics* 2017;33(8):1179-86.

30. Lun AT, Bach K, Marioni JC. Pooling across cells to normalize single-cell RNA sequencing data with many zero counts. *Genome Biol* 2016;17:75.
31. Huber W, Carey VJ, Gentleman R, et al. Orchestrating high-throughput genomic analysis with Bioconductor. *Nat Methods* 2015;12(2):115-21. doi: 10.1038/nmeth.3252
32. Lun AT, McCarthy DJ, Marioni JC. A step-by-step workflow for low-level analysis of single-cell RNA-seq data with Bioconductor. *F1000Res* 2016;5:2122.
33. Dahlin JS, Hamey FK, Pijuan-Sala B, et al. A single-cell hematopoietic landscape resolves 8 lineage trajectories and defects in Kit mutant mice. *Blood* 2018;131(21):e1-e11. doi: 10.1182/blood-2017-12-821413 [published Online First: 2018/03/27]
34. Aibar S, González-Blas CB, Moerman T, et al. SCENIC: single-cell regulatory network inference and clustering. *Nat Methods* 2017;14(11):1083-86.
35. Mease P, Charles-Schoeman C, Cohen S, et al. Incidence of venous and arterial thromboembolic events reported in the tofacitinib rheumatoid arthritis, psoriasis and psoriatic arthritis development programmes and from real-world data. *Ann Rheum Dis* 2020;79(11):1400-13.
36. Dighe AS, Richards E, Old LJ, et al. Enhanced in vivo growth and resistance to rejection of tumor cells expressing dominant negative IFN gamma receptors. *Immunity* 1994;1(6):447-56.
37. Kaplan DH, Shankaran V, Dighe AS, et al. Demonstration of an interferon gamma-dependent tumor surveillance system in immunocompetent mice. *Proc Natl Acad Sci U S A* 1998;95(13):7556-61.
38. Savas P, Virassamy B, Ye C, et al. Single-cell profiling of breast cancer T cells reveals a tissue-resident memory subset associated with improved prognosis. *Nat Med* 2018;24(7):986-93.

39. Edwards J, Wilmott JS, Madore J, et al. CD103(+) Tumor-Resident CD8(+) T Cells Are Associated with Improved Survival in Immunotherapy-Naïve Melanoma Patients and Expand Significantly During Anti-PD-1 Treatment. *Clin Cancer Res* 2018;24(13):3036-45.
40. Shi LZ, Fu T, Guan B, et al. Interdependent IL-7 and IFN-gamma signalling in T-cell controls tumour eradication by combined alpha-CTLA-4+alpha-PD-1 therapy. *Nat Commun* 2016;7:12335.
41. Grasso CS, Tsoi J, Onyshchenko M, et al. Conserved Interferon-gamma Signaling Drives Clinical Response to Immune Checkpoint Blockade Therapy in Melanoma. *Cancer Cell* 2020;38(4):500-15.
42. Gao J, Shi LZ, Zhao H, et al. Loss of IFN-gamma Pathway Genes in Tumor Cells as a Mechanism of Resistance to Anti-CTLA-4 Therapy. *Cell* 2016;167(2):397-404.
43. Zaretsky JM, Garcia-Diaz A, Shin DS, et al. Mutations Associated with Acquired Resistance to PD-1 Blockade in Melanoma. *N Engl J Med* 2016;375(9):819-29.
44. Manguso RT, Pope HW, Zimmer MD, et al. In vivo CRISPR screening identifies Ptpn2 as a cancer immunotherapy target. *Nature* 2017;547(7664):413-18.
45. Sade-Feldman M, Yizhak K, Bjorgaard SL, et al. Defining T Cell States Associated with Response to Checkpoint Immunotherapy in Melanoma. *Cell* 2018;175(4):998-1013.
46. Kalbasi A, Tariveranmoshabad M, Hakimi K, et al. Uncoupling interferon signaling and antigen presentation to overcome immunotherapy resistance due to JAK1 loss in melanoma. *Sci Transl Med* 2020;12(565).

Figure Legends:

figure 1

Study design. ICI = immune checkpoint inhibitor

figure 2

CD8⁺ Tissue resident memory T (T_{RM}) cells predominate in immune checkpoint inhibitor (ICI)-colitis and their activation correlates with endoscopic and histological findings. Mononuclear cells from colonic biopsies from healthy volunteers (HV; N=8), active UC (N=7), anti-CTLA-4/PD-1 “dual checkpoint inhibitor colitis” DCC (N=12) and anti-CTLA-4/PD-1 treated with no colitis (DCNC; N=8). Flow cytometry demonstrates **Ai-iii** DCC is associated with a CD3⁺ T cell lymphocytosis, and CD8⁺ T cells predominance. **iv-vi**

The majority of CD8⁺ T cells express tissue-residency marker CD103, with higher activation in colitis than CD8⁺CD103⁻ counterparts. **vii-viii** The proportion of CD8⁺CD69⁺CD103⁺ T_{RM} cells does not significantly differ across disease states, however activation is highest in the DCC group. **P* < .02, ***P* < .01, ****P* < .001 and *****P* < .0001 by Mann-Whitney test with Bonferroni correction. **ix** Co-expression of activation markers CD38 and HLA-DR are highest in patients with UC and DCC with CD8⁺CD69⁺CD103⁺ T_{RM} cells (*red*) displaying higher expression of these markers than CD8⁺CD103⁻ non-resident T cells (*blue*). Live CD45⁺CD8⁺ T cells are shown. **B** Proportion of activated CD8⁺ T_{RM} cells positively correlates with anti-CTLA-4/PD-1-colitis severity and measured by UCEIS (Spearman's correlation). **C** Multiplexed spectral microscopy of a patient with DCC. Co-localisation of CD3, CD8 and CD103 is demonstrated in both gastrointestinal crypts and in the lamina propria. *CK= Cytokeratin, DAPI= 4',6-diamidino-2-phenylindole nuclear stain. Data representative of three experiments. **D** Live, singlet CD45⁺CD3⁺ T cells are displayed. **I** Cellular activation of T cells (top right quadrant) in healthy stomach and patients with anti-CTLA-4/PD-1 gastritis. In both health and anti-CTLA-4/PD-1 gastritis the majority of T cells are **ii** CD8⁺ with **iii** T_{RM} cell phenotype. **iv** Increased cellular activation is present in anti-CTLA-4/PD-1 gastritis compared with healthy stomach.*

figure 3

Targeted gene panel analysis of ICI-colitis include unique and common features compared with Ulcerative Colitis and high expression of the IFN- γ signalling pathway.

780-gene Nanostring analysis of colonic biopsy RNA from healthy volunteers (HV; N=8), active UC (N=5), anti-CTLA-4/PD-1 colitis (DCC ; N=9) and anti-CTLA-4/PD-1 treated with no colitis (DCNC; N=8). **A** Heatmap of top 50 differentially expressed genes **B** Number of genes up-regulated ≥ 2 -fold as compared to HV demonstrates 173 of up-regulated genes in

DCC, only 12/173 are also up-regulated in the DCNC group (limited on-treatment effect). 144/173 genes are common between DCC and UC, 28/173 genes are unique to DCC. **C** Manhattan plot indicating significantly upregulated pathways including Response to IFN γ . The complete list is provided in Supplementary Table IV. **D** RNA expression of canonical markers of IFN γ signalling JAK1, JAK2, STAT1 and STAT2 are higher in DCC and UC groups compared with Healthy controls and DCNC groups. $**P < .01$ and $***P < .001$ by 1-way ANOVA.

figure 4

Bulk RNASeq analysis confirms anti-CTLA-4/PD-1-colitis has a transcriptome distinct from UC with IFN- γ signalling stronger than TNF- α signalling.

Bulk RNASeq data generated from total RNA extracted from patients with anti-CTLA-4/PD-1 “dual checkpoint inhibitor colitis” (DCC), those with active UC and healthy volunteers (HV) are shown. **A** Partial least squares-discriminate analysis (PLS-DA) demonstrate the divergent transcriptome of DCC and UC, **B** Module Enrichment analysis demonstrated over-expression of hallmark gene “modules” 3 and 4 in DCC, **C** Over representation Analysis demonstrates the over-represented genesets in Modules 1, 3 and 4. Over-expressed pathways include *IFNG* signalling (box), which was more highly expressed than TNF- α signalling. **D** Co-expression and interaction of genes in Module 1, 3 and 4 as determined by Biological General Repository using Interaction Datasets (BioGRID). *Co-expressed genes=blue, gene interaction=brown, gene co-expression and interaction=green.*

figure 5

CD8⁺ T_{RM} cells in ICI-colitis express high proportions of checkpoint inhibitors, cellular activation/cytotoxicity markers and *IFNG*. Single cell RNASeq analysis of 5, 876 cells

from healthy volunteers (HV; N=3), active UC (N=2), anti-CTLA-4/PD-1 colitis (DCC; N=3), anti-CTLA-4/PD-1 treated with no colitis (DCNC ; N=3), PD-1 colitis (PDC; N=2) and PD-1 treated with no colitis (PDNC; N=3). **A** t-stochastic neighbour embedding (t-SNE) projection of live CD45⁺ lymphocytes formed 8 transcriptionally distinct clusters. **B** Proportion of clusters formed from cells from each disease state, with Cluster 4 (box) most common in DCC. **C** Canonical gene markers of each clusters used to define annotation with Cluster 4 (box) expressing CD3, CD8, CD69 and CD103 consistent with Tissue Resident Memory T (T_{RM}) cells. **D** High expression of immune checkpoint molecules on (Cluster 4) CD8⁺ T_{RM} cells (box). **E** t-SNE projection of T cells, highlighted by patient group. **F** Distribution of CD8⁺ T_{RM} cells as shown by cells co-expressing *CD8*, *CD69* and *ITGAE(CD103)* in pink (low expression) red (high expression). **G** Histogram showing cells that express a canonical gene-set list for T cells (dark blue) were selected from the total data for analysis in E,F,G,H,I and K. **H** Expression of activation markers *HLADR*, *GZMB*, *PRF1* and *CD38* (to a lesser extent) overlap with the CD8⁺ T_{RM} cell zone. **I** Expression of *IFNG* overlaps with the CD8⁺ T_{RM} cell zone with *IFNG* being detected in UC, DCC and PDC groups. **J** Heatmap based on all CD45⁺ cells showing the most differentially expressed genes in each patient group. **K** Heatmap based on T cells only showing differential expression between *ITGAE(CD103)*⁺ and *ITGAE*⁻ cells.

figure 6

CD8⁺ Tissue resident memory T (T_{RM}) cells express high levels of *IFNG* in PD-1-associated colitis. Data from a single cell protein and RNASeq analysis of 23,265 gut-derived T cells from healthy volunteers (HV; N=4), patients with active UC (N=3), PD-1 colitis (PDC ; N=5) and PD-1 treated with no colitis (PDNC; N=2). **A** t-stochastic neighbour embedding (t-SNE) projection of live T cells formed 7 distinct clusters. t-SNE plots of all

groups showing expression of **B** *CD4* **C** *CD8A* **D** *ITGAE*(CD103) **E** Distribution of CD8⁺ T_{RM} cells as shown by cells co-expressing *CD8*, *CD69* and *ITGAE*(CD103) in pink (low expression) and red (high expression). **F** Expression of *IFNG* is shown in All Groups, displaying overlap with CD8⁺ T_{RM} cell zones **G** Distribution of cells based on patient groups demonstrates T cells from patients with PDC are found predominantly in the CD8⁺ T_{RM} cell zones (Cluster 1 and 6). **H** Heatmap based on CD8⁺ T_{RM} cell Populations 1-3 only displaying top differentially expressed genes.

figure 7

Tofacitinib results in rapid resolution of treatment-refractory ICI-colitis, and correlates with resolution of CD8⁺ T_{RM} cell activation and down-regulation of JAK/STAT signalling.

A Clinical time-course of a 61M with non-small-cell lung cancer treated with carboplatin, pemetrexed and pembrolizumab. The anti-PD-1-colitis was refractory to multiple therapies. Tofacitinib resulted in prompt resolution of clinical symptoms, and endoscopic and histopathology inflammation. Tofacitinib was continued for six weeks. *Star*= crypt abscess, *Thick arrow*=attenuated crypt, *Thin arrow*= crypt architectural distortion, *triangle*=erosion.

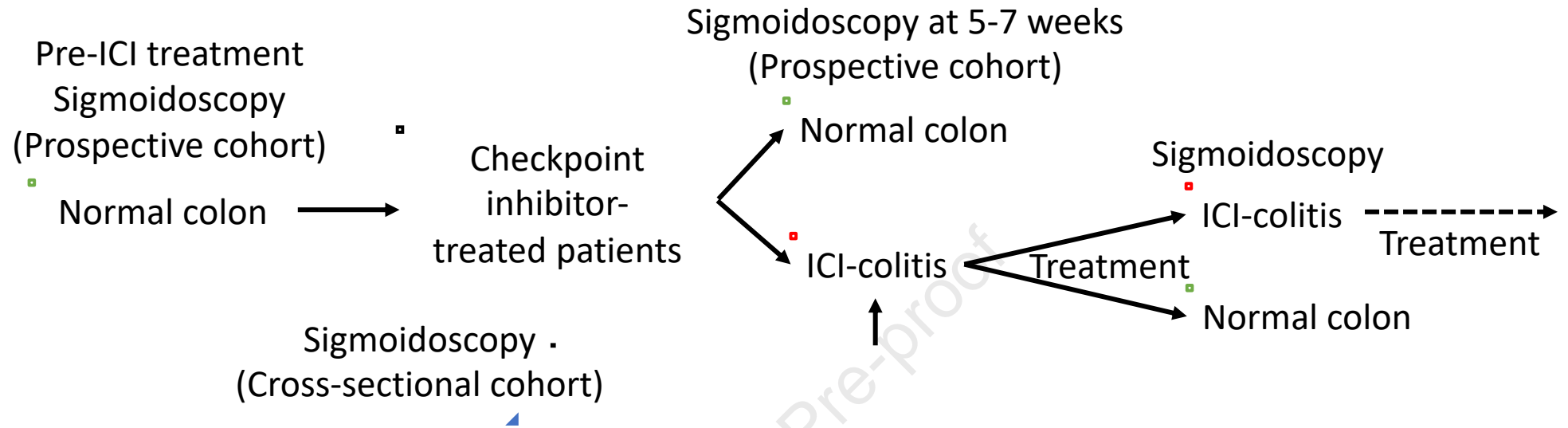
B Fecal microbiota transplant (FMT) response in a previous ICI-colitis patient, where clinical resolution was associated with normalisation of CD8⁺ T_{RM} cell activation. Flow cytometry gated on live CD3⁺CD8⁺CD69⁺CD103⁺ T_{RM} cells. **C** Utilising the same donor stool, FMT did not result in resolution of clinical symptoms or resolution of CD8⁺ T_{RM} cell activation in this 61M who subsequently received tofacitinib. **D** Flow cytometry plots gated on live single CD45⁺CD3⁺ T cells are shown. Prior to tofacitinib, wide-spread activation of CD4⁺ and CD8⁺ T cells is evident, with the highest level of activation in CD8⁺CD103⁺ T_{RM} cell subset (61%). Following six weeks of tofacitinib, there is resolution of T cell activation including in the CD8⁺CD103⁺ T_{RM} cell subset (7%). **E** Gene Set Enrichment Analysis of bulk RNASeq data

demonstrates *IFNG* signalling pathway enrichment in ICI-colitis. **F** Data from Nanostring RNA-plex assay from the tofacitinib-treated patient, and 3 Healthy Volunteers (HV).

Tofacitinib results in significant downregulation of JAK1, JAK3, STAT1, STAT2, STAT3, STAT4 and STAT5A. $*P < .05$, $**P < .01$, $***P < .001$, $****P < .0001$ and $*****P < .00001$ by *Mann-Whitney test*. **G** Volcano plot depicting pre- and post-tofacitinib.

Journal Pre-proof

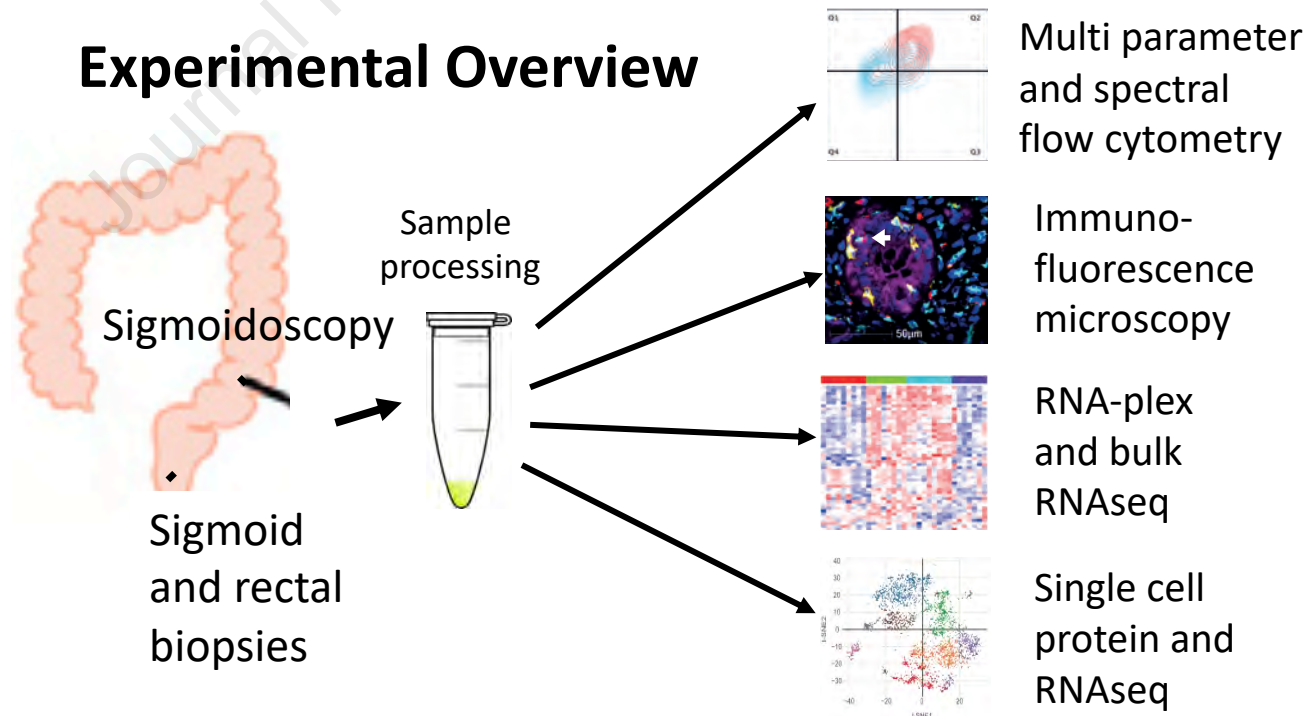
ICI-Treated Patients: Prospective Longitudinal and Cross-Sectional Cohorts

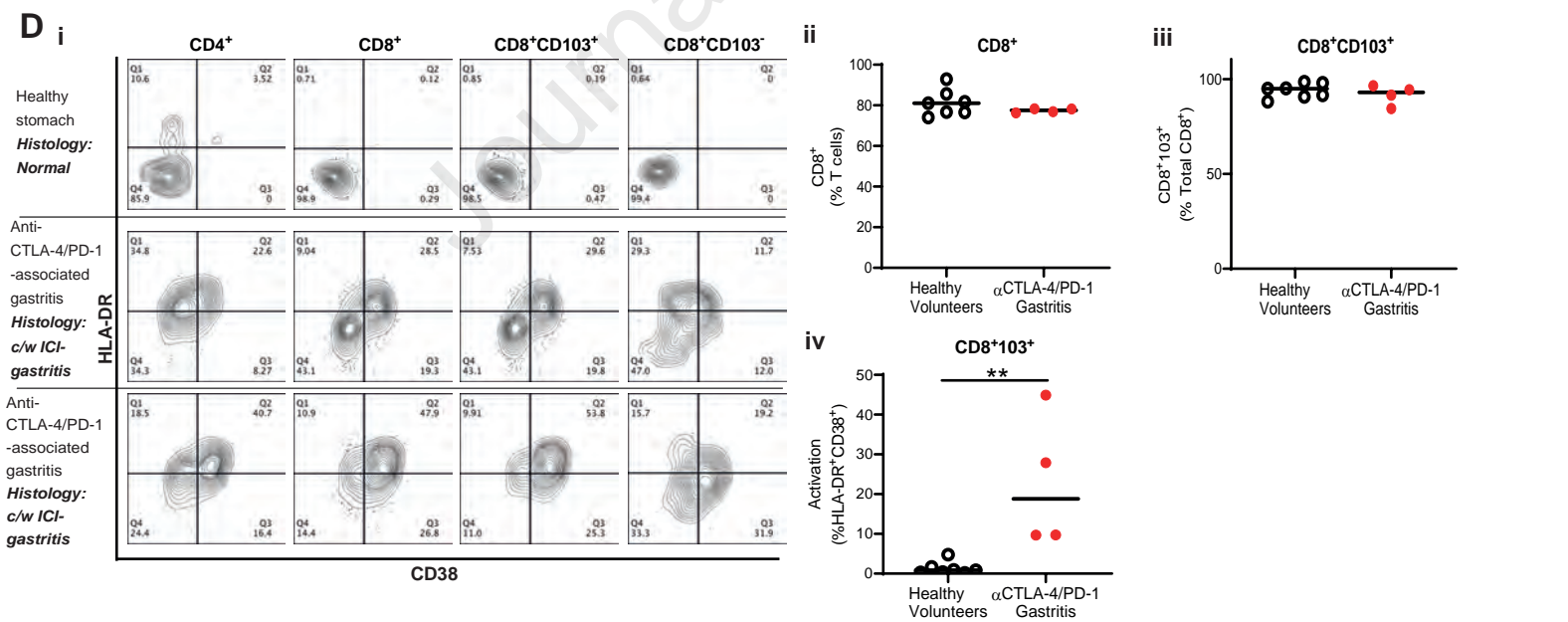
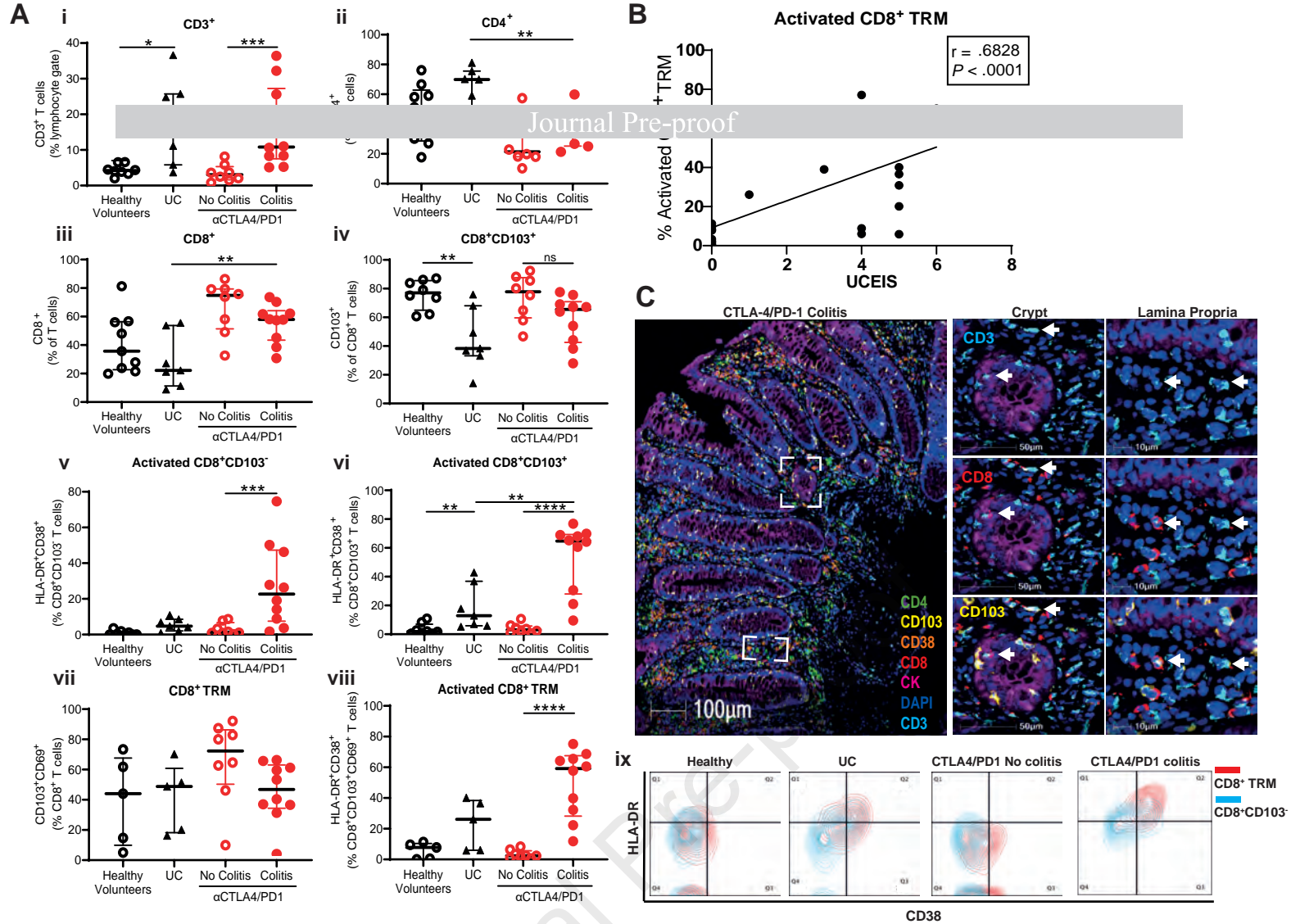


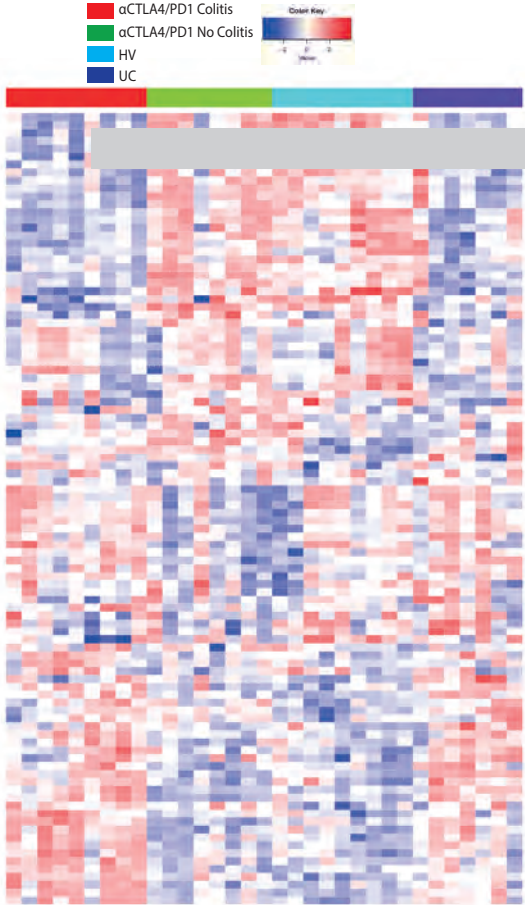
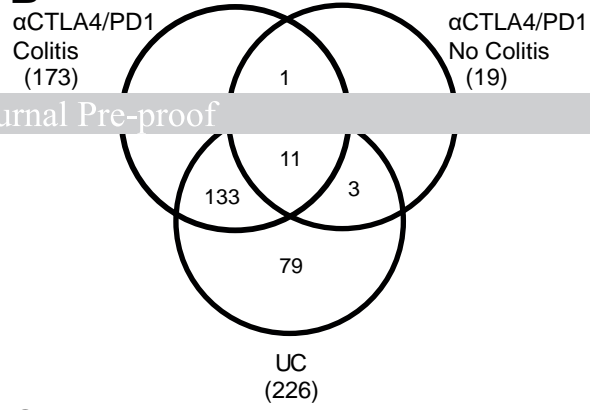
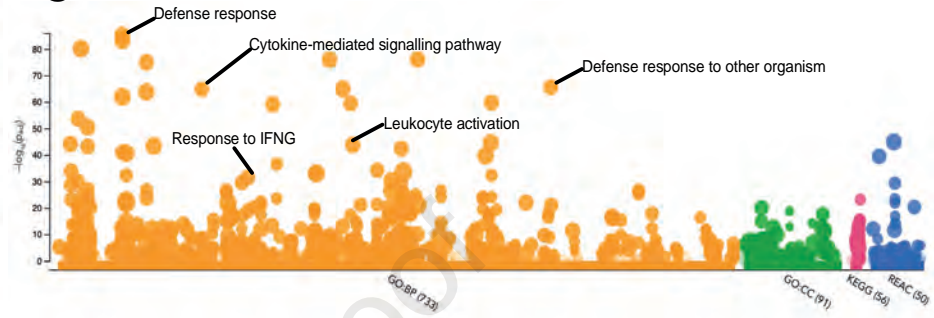
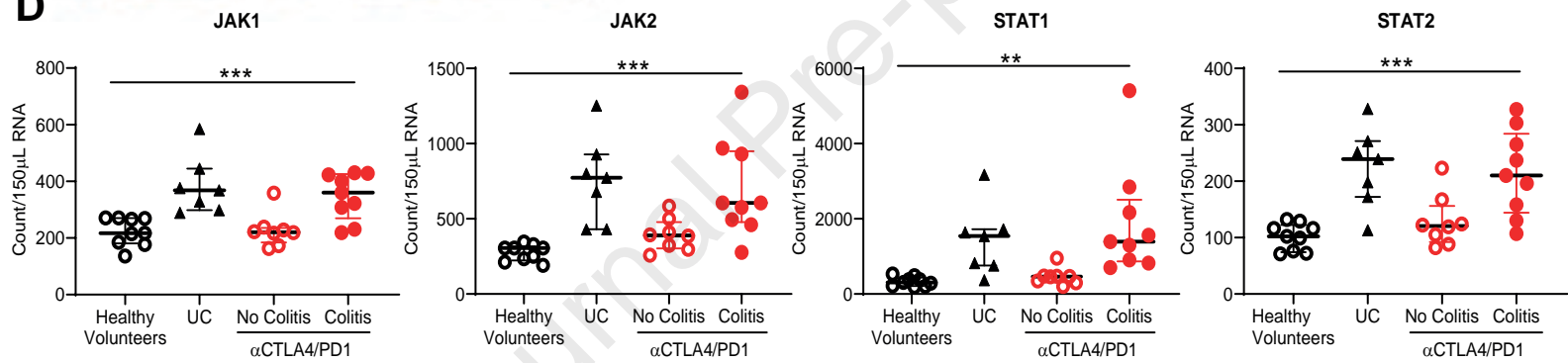
Non-ICI Controls (sigmoidoscopy)

- Healthy controls Normal colon
- Active ulcerative colitis

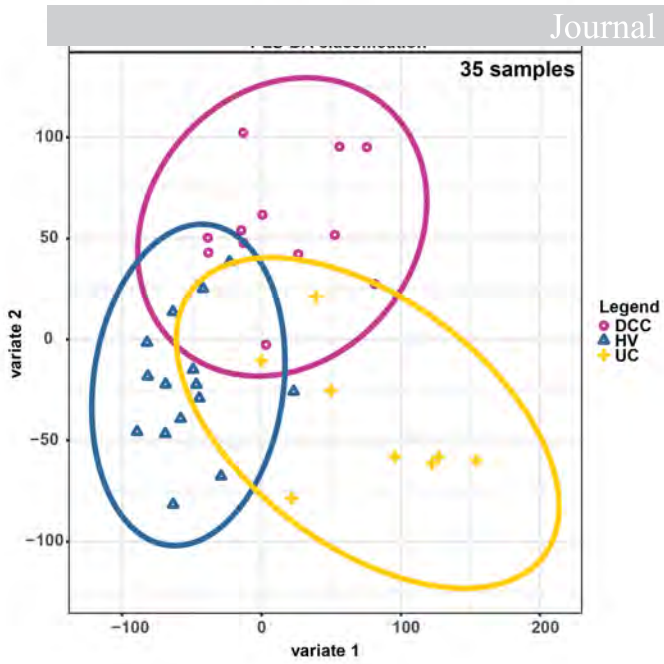
Experimental Overview



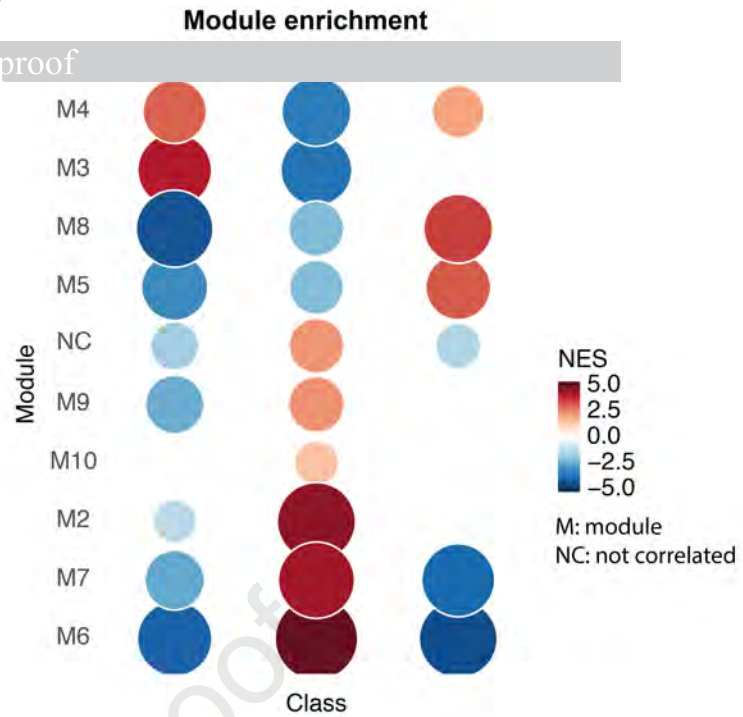


A**B****C****D**

A

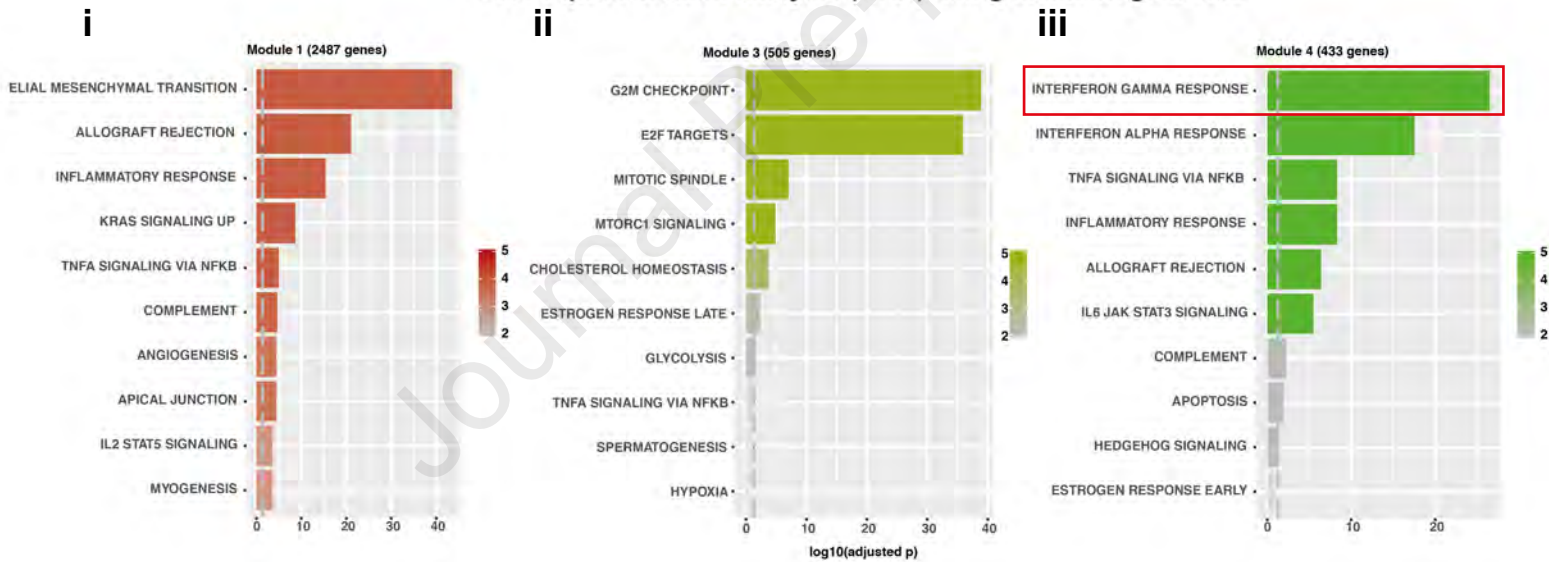


B



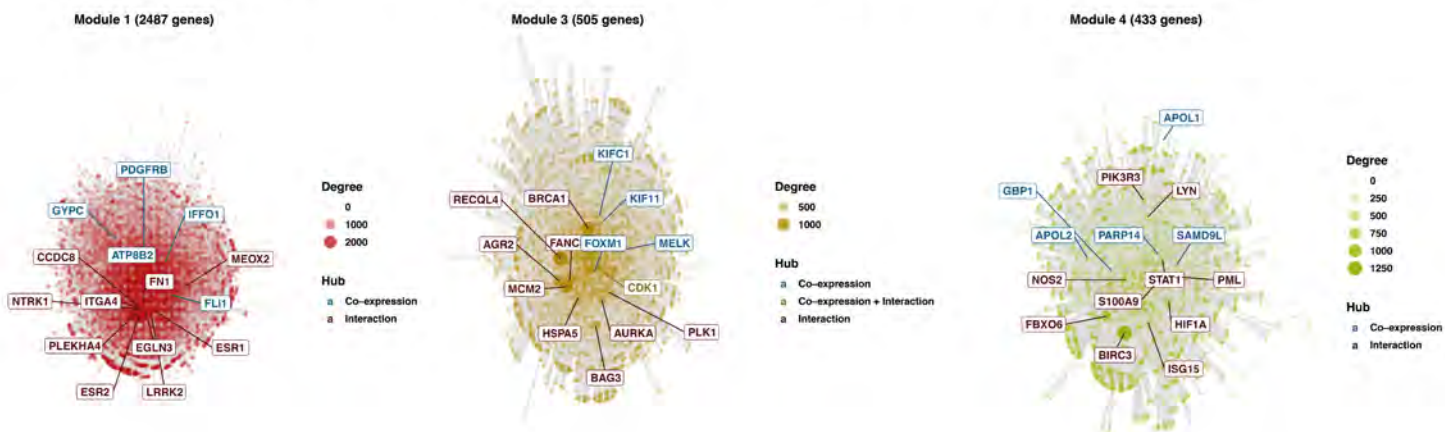
C

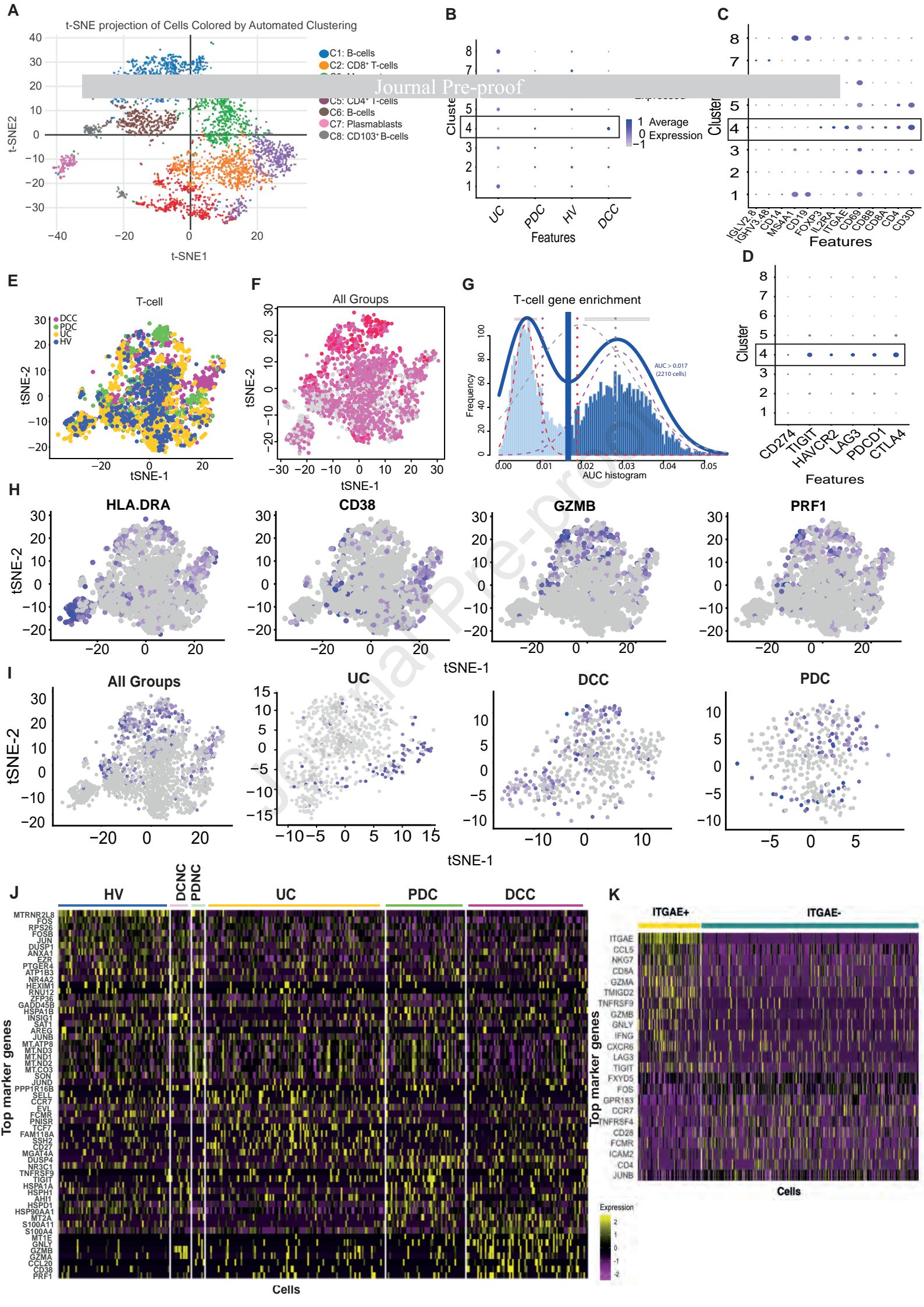
Over representation analysis (ORA) using hallmark gene sets

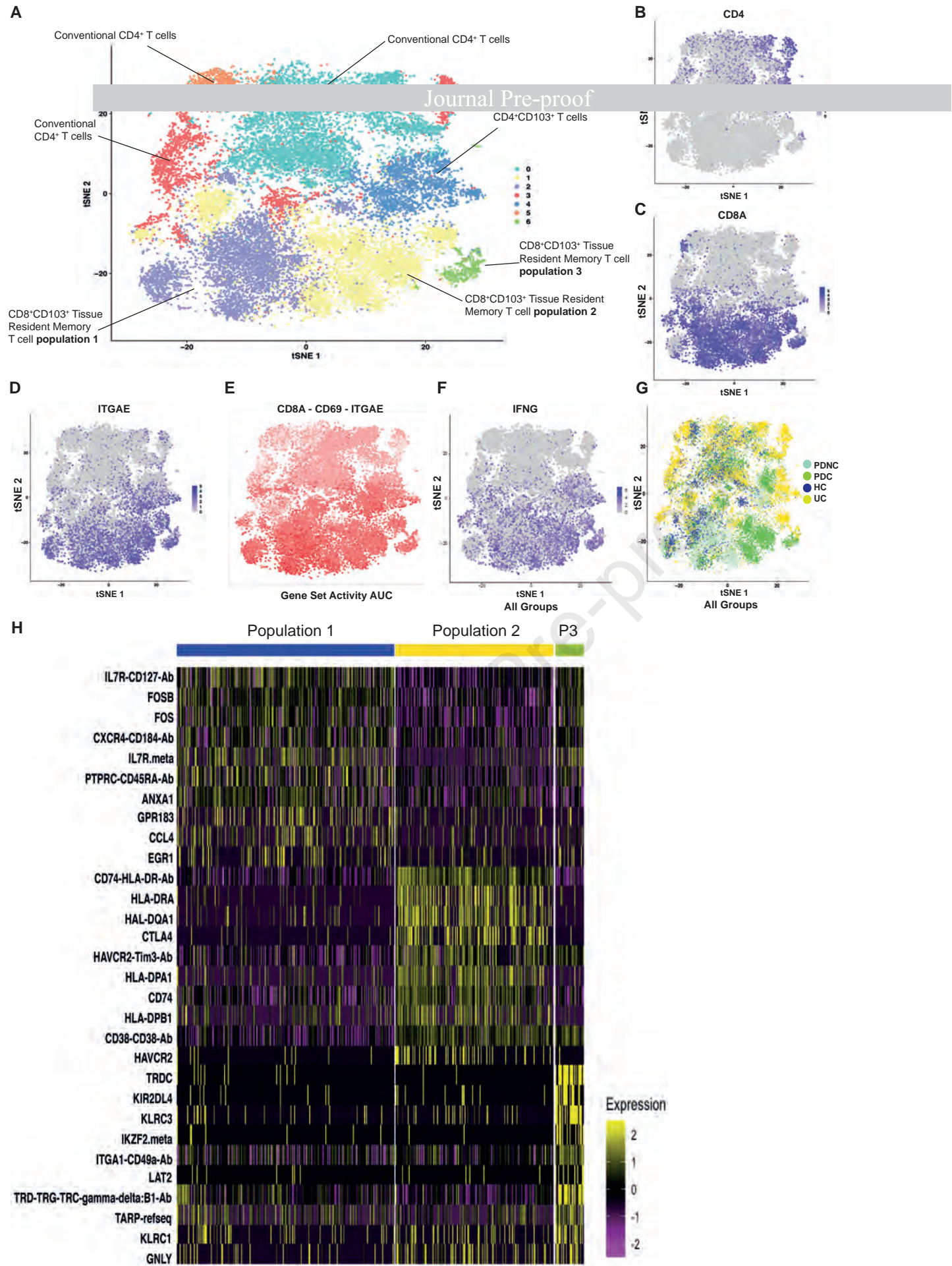


D

Module graphs using Biological General Repository using Interaction Datasets (BioGRID)







What you need to know

Background and context

- ICI-colitis is a common side-effect of checkpoint inhibitors, may mimic inflammatory bowel disease, and currently has empirically-derived treatment guidelines.

New findings

- We identify both unique and overlapping immunopathology in ICI-colitis and UC.
- CD8⁺ T_{RM} are the key effector cells in ICI-colitis. T_{RM} strongly express checkpoint proteins and IFN γ .
- We present the first PD1-inhibitor-associated colitis single cell analysis which demonstrates consistent T_{RM} activation. IFN γ -JAK-STAT activation identified tofacitinib as a potential therapy, although IFN γ blockade could negatively affect oncological response.

Limitations

- This is a small human cohort study. Further investigation will be required to understand the role of the microbiome in T_{RM} activation and the safety of JAK inhibition.

Impact

- This analysis of CD8⁺ T_{RM} and associated immune pathways in ICI-colitis provides a basis for targeted therapy development. We provide an immunologic rationale for the use of JAK inhibitor therapy in refractory ICI-colitis.

Lay Summary

We present an analysis of the immunopathology in checkpoint-inhibitor colitis, a common side-effect of cancer immunotherapy. We utilised our findings to successfully identify a novel therapy for a case of refractory colitis.